THE CAMBRIDGE ELECTRON ACCELERATOR

M. S. LIVINGSTON

Massachusetts Institute of Technology and
Harward University, Cambridge (Mass.)

The Massachusetts Institute of Technology and Harvard University are cooperating in the design, construction and operation of a 6-Bev electron accelerator to be located in Cambridge, Mass., on Harvard University grounds. Funds for the support of this machine are to be provided by the U.S. Atomic Energy Commission as part of their program in support of research in high energy physics in the universities. Preliminary design studies have been supported for the past two years by a joint program of the Office of Naval Research and the Atomic Energy Commission, using the part-time services of about 24 scientists and engineers from Harvard and M.I.T.

Cost of construction, including all buildings and personnel salaries, is estimated to be $6.500,000. The time required to complete construction will be about 4 years. Detailed designing will start by July 1, 1956, and the construction of some of the buildings should be underway by late fall. The responsibility for the construction contract with the Atomic Energy Commission will be assumed by Harvard University. However, a joint management committee of scientists and administrators from both schools will supervise the construction and operation of the accelerator as a research facility. Although the initial authorization provides funds to power the accelerator to 6.0 Bev, the orbit radius has been chosen large enough to allow higher ultimate energy. Future expansion of the power supply is planned to reach 7.5 Bev.

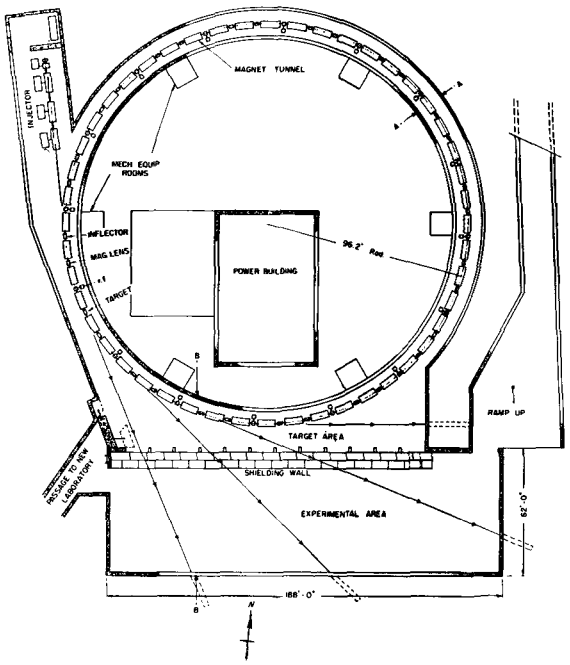

Fig. 1. Plan view of the 6-Bev electron accelerator.

General description

The accelerator will be an electron synchrotron, formed of a ring of 48 strong-focusing magnets utilizing the alternating-gradient principle. Magnet sectors will be spaced by 48 field-free straight sections, each 4 ft long. The magnet circle radius is to be 118 ft and the orbit radius within magnet sectors is 86 ft. The flux density required for 6.0 Bev electrons is 7.6 kilogauss; for 7.5 Bev it will be 9.5 kilogauss. This relatively large orbit radius and low magnetic field is deliberately chosen to reduce the problem of radiation by the orbiting electrons to manageable proportions. Since flux densities are well below the saturation region the design of the magnet is considerably simplified and corrections are minimized.

The AG magnet sectors will be arranged in a sequence described by the code-word "fofdod" (focusing-zero-focusing-defocusing-zero-defocusing), in which the straight sections (zero) are placed in the centers of the gradient sectors. This location involves minimum effect on oscillation amplitudes by straight sections, and simplifies construction. The gradients, or n-values, will be designed to provide 5.4 free oscillation wavelengths per turn, for both radial and vertical free oscillations. We choose to avoid orbital resonances, of the integral, half-integral and sum types, but we use the results of the Brookhaven electron analogue to justify operation on a difference resonance. In this location within the stability "diamond" a variation of $\pm$ 2.5% in average n-value is allowable. Quadrupole lenses in the straight sections will be time-scheduled to provide corrections of the average gradient due to changing magnetic properties, so as to maintain operation within the stability diamond during acceleration.

Each magnet sector will be constructed of laminated iron, as for a transformer, bonded into solid segments

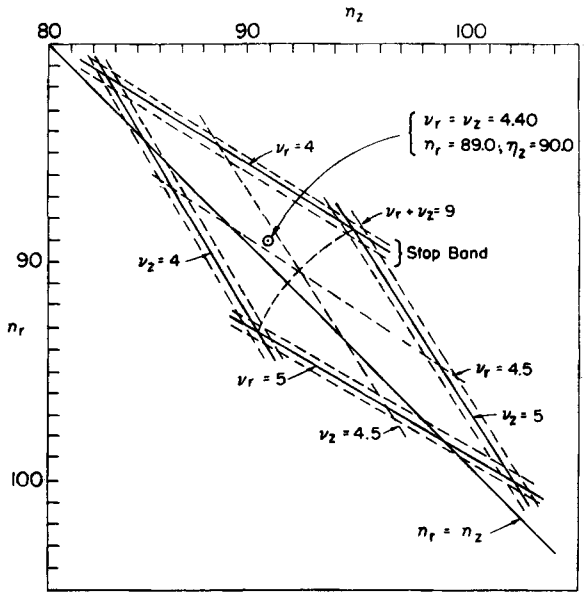

Fig. 2. n-value stability diamond for operation at $\nu_p = \nu_z = 4.40$.

about 4 inches thick for rigidity, and assembled into a rigid structural unit 11 ft long having the orbit radius of curvature. Present plans call for die-stamping the laminations as complete units, with the designed pole-face profile. Half of each sector will have a "positive gradient and half a "negative" gradient. Excitation windings formed in layers to slip between pole tips will enclose the entire sector, formed of water-cooled bus bars and insulated with glass-fibre tape and a polyester resin.

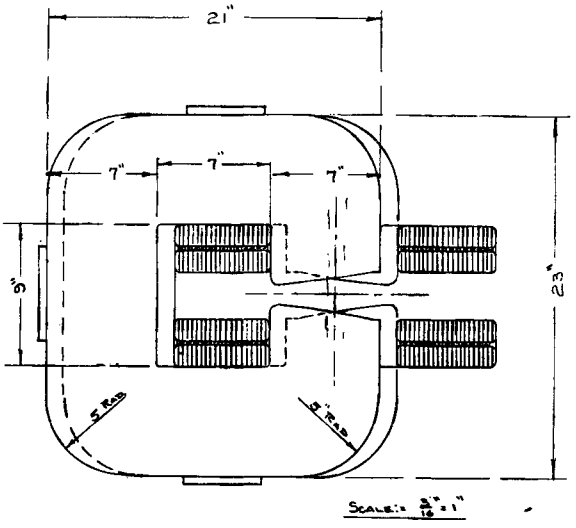

Fig. 3. Cross-section of magnet showing displacement of positive and negative sectors for maximum useful aperture.

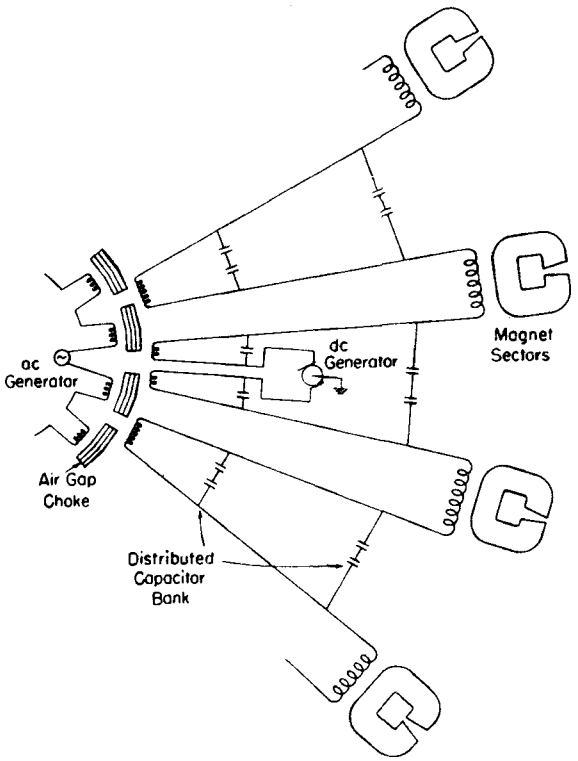

Fig. 4. Magnet power circuit.

The magnet will be excited by a resonant power supply at 30 cycles per second, with a dc bias to give uni-directional pulsing. Parallel resonant circuits for each magnet sector will use capacitors to store energy and transfer it to air-gap chokes during the low-field part of the magnetic cycle. The peak stored energy in the magnetic field (for all 48 sectors) will be about 800,000 joules, and the power required to excite the magnet, including conductor heating and magnetic losses, will be about 400 kW at 6-Bev excitation or 650 kW at 7.5 Bev. Injection will occur near 25 gauss, at a phase of the cycle when the rate of field increase, dB/dt, is low, which minimizes eddy current distortion of the field. The interval for acceleration, during which the field rises to maximum, is 15 milliseconds,

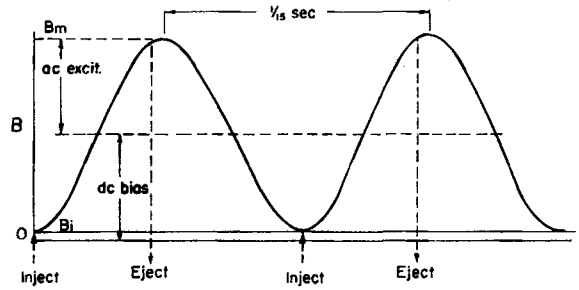

Fig. 5. Magnet excitation cycle, with half-dc-biais.

and the electrons will reach maximum energy in about 20,000 turns.

Radiofrequency accelerating cavities will be located in 16 of the straight sections, driven in phase at a constant frequency of about 500 megacycles, which is a high harmonic (about the 350th) of the orbital frequency. This use of high harmonic order reduces the dimensions of the cavities and so lowers the circulating electrical energy and rf losses. It also reduces synchronous oscillation amplitude. The maximum rate of acceleration, at half-excitation, is 0.4 Mev per turn.

Energy loss due to radiation by the beam increases with the 4th power of particle energy, reaching 4.4 Mev per turn per electron at 6 Bev and 10.7 Mev per turn at 7.5 Bev. These peak values occur at the end of the acceleration cycle and set the volts-per-turn requirement. For perspective it might be pointed out that the 16 cavities represent a spaced linear accelerator of about 40 ft. total length; an output energy of 10.7 Mev in a 40 ft. linear accelerator is well within current practice.

Each cavity will be a drift-tube-loaded resonant system, with 2 (or possibly 3) accelerating gaps between drift tubes depending on choice of frequency, and will look like a short section of a linear accelerator, about 2.5 ft. long and 18 inches diameter. An outer vacuum tank will enclose the copper cavity, which will be water-cooled for thermal stability. For such a resonant cavity we estimate an electrical efficiency Q of 30,000 and a shunt impedance of 10 megohms.

The peak voltage requirement per cavity, of about 1 million volts sets the peak power requirement for the radiofrequency amplifiers. A more demanding requirement is the average power, to supply cavity losses and beam load during the long (nearly 50%) rf duty cycle. Beam load will represent about half of the total power. Present plans call for klystron amplifiers delivering a peak power of 25 kVA and an average power of 5 kW per cavity at 6 Bev, or a peak of 75 kVA and an average of 12 kW per cavity at 7.5 Bev. The total dc power needed to supply the klystrons will be about 750 kW at 7.5 Bev.

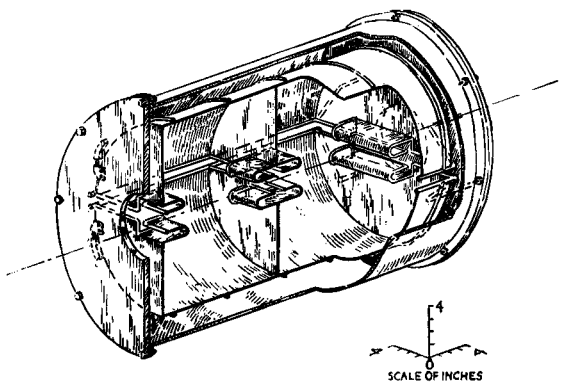

Fig. 6. Cut-away view of radiofrequency accelerating cavity.

Electrons will be accelerated initially to about 20 Mev in a linear accelerator, operating at a frequency which is preferably an integral multiple of the synchrotron rf frequency. At this energy the velocity defect will shift the equilibrium orbit inward only 0.4 inch. The angular spread of the linear beam, estimated as $\pm$ 1 $\times$ 10^{-3} radians, will cause betatron amplitudes in the AG magnet field of about $\pm$ 0.4 inches. However, the energy spread of $\pm$ 0.5 Mev will produce a radial spread in equilibrium orbits up to $\pm$ 1.5 inches. We anticipate some loss in beam due to this energy spread, and hope to develop an energy-bunching system to reduce it.

An electrostatic inflecting field in one straight section will direct the linear beam into the central orbit, with the pulse timed to match the magnetic field for injection. This inflecting field will be pulsed off in a time short compared with the 0.75 microsecond orbital period, filling essentially one turn. We estimate that with a pulse current of 0.25 amperes from the linear accelerator, about 1 $\times$ 10^{12} electrons will be injected into the orbit. Orbit acceptance in the 5 inch $\times$ 1.5 inch vacuum chamber, and phase acceptance into synchronous orbits will reduce the number captured to about 2 $\times$ 10^{11} per pulse, which should then be accelerated to high energy.

The anticipated output beam intensity, at 30 pulses per second, is 6 $\times$ 10^{12} electrons per second, a time-average current of 1 microampere. At 6 Bev energy this represents a beam power of 6 kilowatts, which can be compared with about 16 kilowatts radiated during acceleration.

We will now discuss some of the special features which have been analyzed during design, and present some preliminary results from magnet model studies.

Phase modulated injection

The intensities described above represent expected values from a free-running linear injector and suffer losses due to the phase acceptance limitation of the synchrotron. We propose to increase the intensity of electrons captured in synchronous orbits by phase modulating the injector. For example, if the linear accelerator is designed to operate at a frequency which is an integral multiple of the synchronous radiofrequency, such as 1000 Mc ($\times$ 2) or 3000 Mc ($\times$ 6), the output beam of the linear machine will be pre-bunched in phase, with a phase spread which is narrow compared with the phase acceptance of the synchrotron. Furthermore, if the input to the linear accelerator (at the electron gun) is modulated at the synchronous frequency, a single pulse of electrons will be accelerated for each synchrotron cycle. The modulated output of the linear machine can have much higher peak current, for the same power input, increasing the intensity of the useful beam injected into the synchrotron by a factor of 2 or more. Another useful result is the reduction of initial synchronous radial oscillations associated with energy oscillations in the synchrotron.

To accomplish this result the linear accelerator will be driven at a harmonic of the synchrotron frequency, from a common master oscillator, with relative phasing controls to determine the phase of pulse injection. The type of modulation required for the linear machine will be determined after suitable power tubes and frequencies are chosen. Beam loading of the rf cavities for such increased intensities exceeds the capacity of the designed rf power supply. Higher intensity will require an increase in rf power, which sets the intensity limit for this type of accelerator.

Phase modulation represents an attempt to match the properties of the injector to those of the accelerator. It has a more general application than just to this electron machine, and might be considered to advantage for other accelerator systems.

Magnet alignment

We have conceived a technique for magnet alignment using the electron beam called "one-turn alignment", which should relax mechanical alignment requirements and also provide a method of correcting deviations from alignment during operation. This is based on a theoretical study of oscillation amplitudes due to misalignments and a conclusion that the maximum deviation Δx in one turn in our AC magnet system will grow to no more than about $2 \Delta x$ in a large number of turns.

We propose to inject a sequence of extremely short pulses of electrons from the linear beam, with a steady inflecting field and a steady magnetic field, and to explore the particle trajectory in the first turn. Available high quality surveying techniques should be sufficient to keep the beam within the chamber during one turn, although possibly with large amplitude deviations. We propose to study the effect on beam trajectory of all types of magnet misalignments, in sufficient detail to be able to recognize and identify the consequences of any single type. With this information it should be possible to correct all major deviations by observing the trajectory, and through a series of corrections to reduce amplitudes below the desired Δx.

The technical features required are a set of 48 pairs of "sensing" electrodes in the straight sections, each of which will provide a differential pulse signal when the electron pulse passes to show the radial (or vertical) deviation. A cathode-ray tube presentation of these signals will show beam location and oscillation amplitudes around the orbit. Suitable controls on magnet alignment screws (possibly motor driven) should make it possible to perform the indicated adjustments, with the effects observable on the C.R.T. With such techniques we believe the magnets can be brought into alignment with a reasonably small effort. Eddy curent and other effects due to dynamic pulsing will of course have to be corrected separately.

Radiation-induced oscillations

During the design study a new and fundamental problem of an AG machine has been recognized and analyzed. This is the growth of oscillations due to the difference in radiation energy loss on the inside and outside of the equilibrium orbit location. The electron radiation has a purely classical energy distribution, extending up to a characteristic energy of about 30 kilovolts. Emission of quanta of these energies exerts a small but finite effect on the amplitude of electron oscillations. Consider an orbit with a residual betatron oscillation. When radiation occurs, the location of the equilibrium orbit jumps instantaneously inward. The electron will radiate more where it has a small radius of curvature, i.e., on the outside of the equilibrium orbit, and less when inside the equilibrium position. This results in a net increase in the amplitude of the betatron oscillation, an antidamping effect. We estimate that some beam loss due to amplitudes exceeding the uniform field region would start at about 5 Bev and might become serious at 6 Bev.

Several techniques are available to provide positive damping sufficient to overcome the amplitude build-up at high energies. For example, a radial gradient in the accelerating electric field might be provided by slanting the faces of the rf gaps in some of the accelerating cavities; this could add energy at a different rate for particles inside and outside the equilibrium orbit, providing damping for betatron oscillations. Another method might be to provide special correcting magnets in straight sections which would induce greater radiation for particles on the inside of the orbit and so compensate for the anti-damping effect. Such a magnet would have equal-length sections of opposed field, to give zero angular deviation, but with both sections formed with a negative gradient so the local orbit curvature is greatest at small radii. Other techniques are possible such as coupling radial and vertical betatron oscillations which would cancel the antidamping effect.

In addition to the classical effect described above another source of induced oscillations at high energy comes from the quantum nature of the radiation. Emission of quanta of these energies will produce a statistical build-up of oscillation amplitudes, both betatron and synchronous. For our conditions this is computed to lead to a radial amplitude of several inches by the time the particles reach 6 Bev energy, if no damping were provided. The damping systems described above are sufficient to limit this increase to a few millimeters while also compensating for the classical build-up effect. The phase amplitude of the synchronous oscillations due to the quantum effect is a more serious limitation. Phase oscillations would grow to about 25° (rms) in phase by 6 Bev, requiring a smaller synchronous phase angle and higher peak rf voltage.

Magnet model studies

A full-scale section of the magnet has been constructed, using the chosen 2-inch gap at the central orbit, with

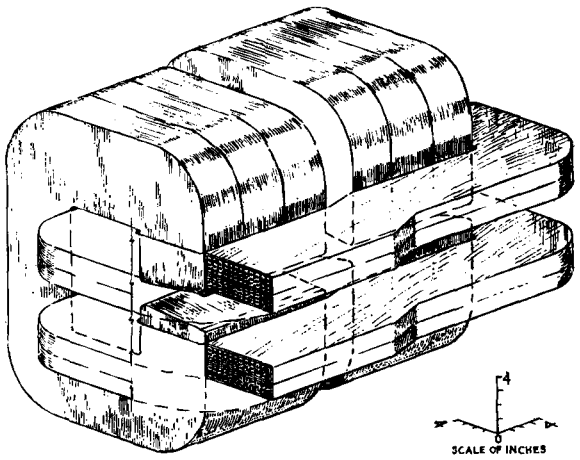

Fig. 7. Illustration of magnet model assembly.

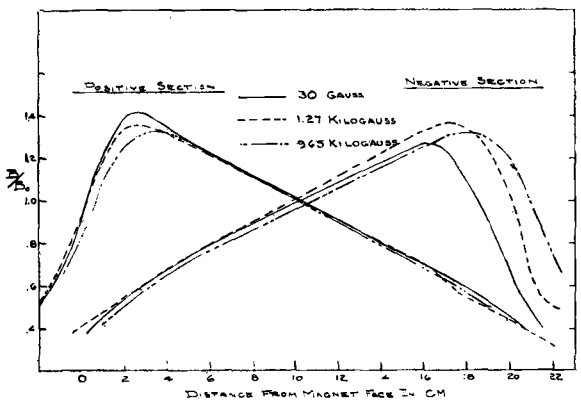

Fig. 9. Magnetic field plots for positive and negative sectors at several values of excitation.

1 ft. of positive gradient and 1 ft. of negative gradient. Excitation coils have the approximate shape planned for the final magnet. It was formed of 0.025 inch Electrical Grade silicon steel; each lamination was coated with insulation; the laminations were bonded by adhesives into solid blocks 4 inches thick. Pole faces were precisely machined to a hyperbolic shape with a constant, $K = 7.95$ in^2, designed to give an n-value of 100 at the chosen orbit radius (present plans would increase this to about 116 and would use larger orbit radius). The central 6-inch width of the 7-inch pole face follows the hyperbolic curve, with a $\frac{1}{2}$ inch round at the nose and a $\frac{1}{2}$ inch flat at the wide side of the gap for edge corrections.

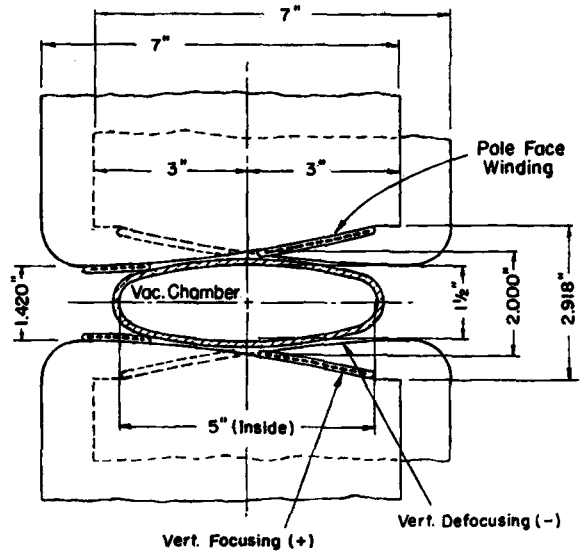

Fig. 8. Model pole face shape, vacuum chamber and pole-face windings.

Measurements made to date include only dc field plots and excitation studies. An ac power supply for dynamic tests is under construction. A variety of instruments have been used, with a relative precision of 0.5% and an absolute calibration of 1 to 2%. Further details are available in a laboratory report.

Radial plots across the field on the median plane show a wider region of uniform-gradient than anticipated. Over the entire excitation range between 500 gauss and 9.5 kilogauss the uniform ($\pm 0.5\%$) region was over $4\frac{1}{2}$ inches wide. At injection field (25 gauss) it was $5\frac{1}{2}$ inches wide. In order to utilize the full effective width we have displaced the two parts of the magnet radially by 1 inch, so the equilibrium orbit is near the center of the uniform-gradient region in both sectors.

Gradients measured in the radial plots are the same as the computed values, within the accuracy of the measurements, for both types of sector. Slight differences between sectors have been noted which may prove to be significant with better precision, and which may be a consequence of the back-leg asymmetry. Extension of the radial

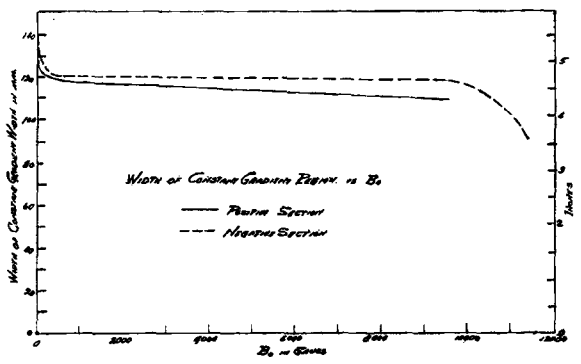

Fig. 10. Plot of width (in mm.) of the constant-gradient field region between poles of 7 inch width.

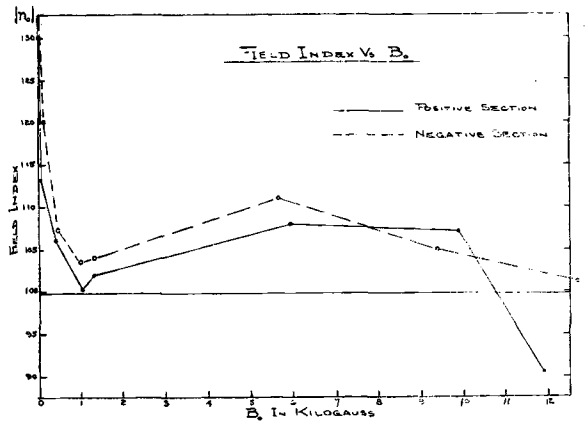

Fig. 11. Variation of n-value with magnet excitation.

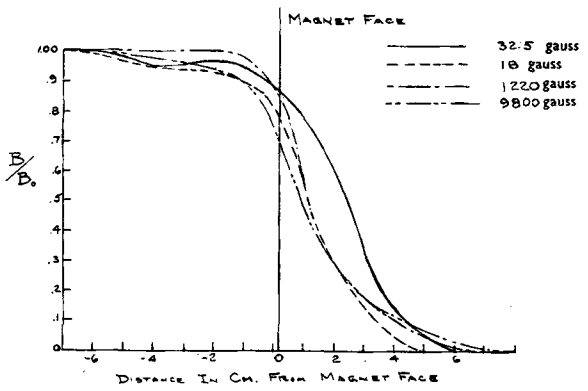

Fig. 13. End fringing field of negative sector.

plots to higher excitation (maximum 11.4 kilogauss) shows a decrease below the computed gradients of about 3%. We have not powered the magnet to saturation and find that the required excitation (ampere-turns per gauss) is only 3% larger at 9.5 kilogauss than at low fields.

The remanent field at the central orbit following full uni-directional excitation is measured to be 19 gauss in both sectors. (This might be reduced by using iron with a higher silicon content.) Radial plots of the remanent field show the same width of uniform-gradient region as at injection field, and with only slightly higher n-values. We are greatly encouraged by observing this uniform-gradient remanent field, and believe that remanent field effects will not distort the radial field distribution.

Extension of fields into the straight sections at sector ends has been studied with some care. The location of the "magnetic face" of the magnet (the position dividing the fringing field into equal areas on a B vs z plot) varies considerably with excitation. At injection field the magnetic face on the central orbit is close to the physical face; at 1500 gauss it is 1.3 inches outside the physical face; at 9.5 kilogauss it has withdrawn to 1.0 inches. Other plots at different radial and off the median plane show the shape of the end fringing field. We intend to use these plots to determine the amount of non-uniform gradient at different radii, and so to predict the change in location of the working point within the stability diamond. The location of the magnetic face at full excitation will be used to determine basic AG magnet parameters; deviations at lower fields can be corrected by using the quadrupole lenses in the straight sections.

A preliminary conclusion from these dc measurements is that the radial field patterns are sufficiently uniform to maintain operation within the stability diamond by using only quadrupole lenses for corrections of average gradient. Dynamic measurements may show the need for some time-scheduled variation of radial field. If so, we plan to use pole face windings cemented to the poles.

Building plans and shielding arrangements

We plan to place the accelerator in a covered trench, with the beam 10 ft. below ground level. The tunnel roof

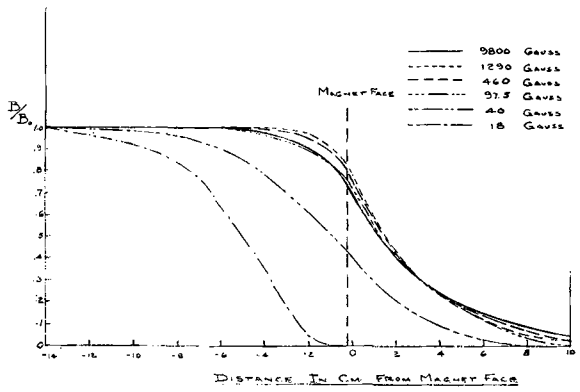

Fig. 12. End fringing field of positive sector, showing the change in effective length of magnet with excitation.

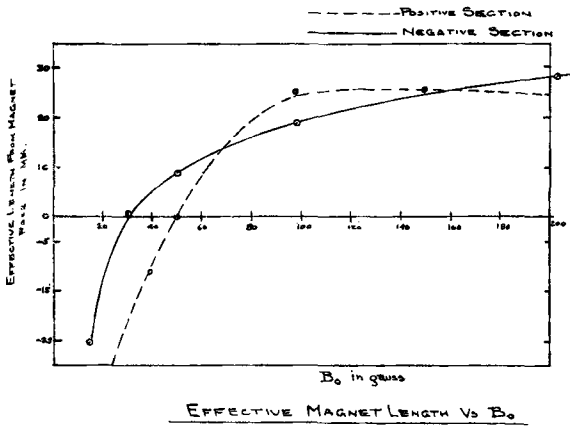

Fig. 14. Variation of effective magnet length with excitation, from remanent field (18 gauss) to 200 gauss.

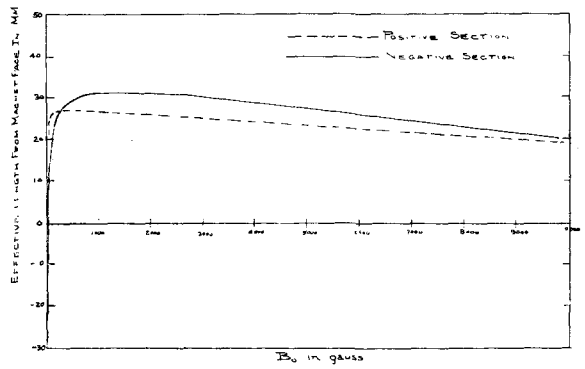

Fig. 15. Variation of effective magnet length with excitation up to 10 kiligauss central field.

will be covered by 4 ft. of earth, increased to 8 ft. over the target area where radiation intensities will be greatest. Our calculations of the excepted intensity of secondary radiations show that the chief component coming through the tunnel roof will be relatively low energy (< 200 Mev) neutrons. The shielding thickness is estimated to keep external intensities well below tolerance levels for all normal operations.

A large experimental area will be provided on one side of the orbit, behind a 10-ft. shielding wall. Beams of gamma rays and other radiations from 3 or 4 alternative target locations will be brought through channels in this wall. Magnetic analysis in the target area inside the wall can be used to separate beams of charged particles, and focusing magnets can be located in this region. The experimental area behind the wall will be about 60 ft. × 200 ft., large enough to allow the permanent installation of 10 or major research installations, and with a beam run over 100 ft. in length in some directions.

The shielding wall will be graded in density, with a 1 ft. layer of steel plate at beam level. The sharply-directional electron-gamma ray showers and the high energy nuclear components of the radiation will be con-

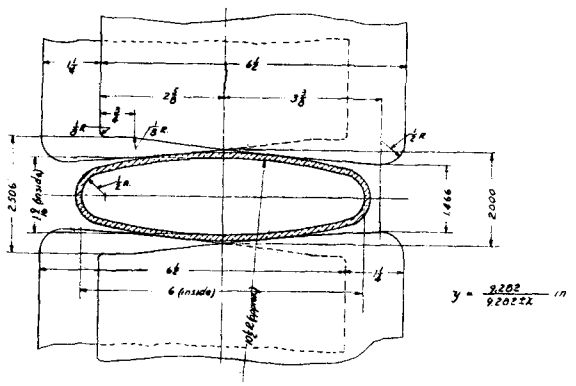

Fig. 16. Revised pole face shape for Model 2.

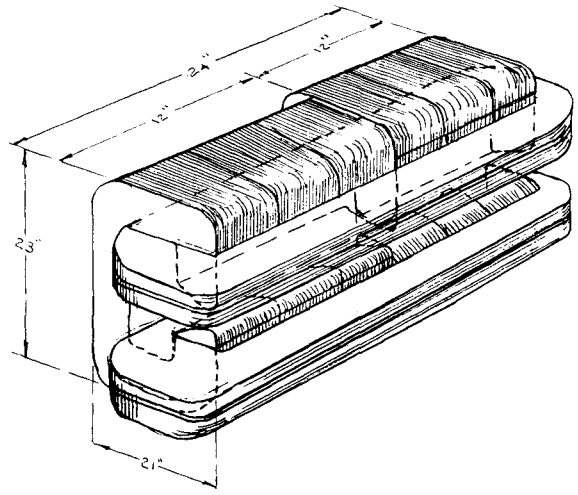

Fig. 17. Illustration of Model 2.

tained within this central steel band. Above and below the steel plates will be iron-loaded concrete blocks; at still wider angles normal concrete blocks will be used. Nuclear components making wider angles with the beam will be of lower energy than those in the forward direction. So less density is required. The widest-angle component is neutrons, for which normal concrete is best. Attenuation calculations show the wall will be sufficient to reduce intensity levels below tolerance with all holes plugged. However, when beam channels are opened the intensity in the experimental area will exceed tolerance and local shielding will be required, strongly dependent on the type of experimental target. If necessary, personnel will be vacated to remote observing stations in the laboratory building.

Research program

The scientific justification of this accelerator is primarily to explore a region of energy of the order of six times higher than will have been reached with beams of electrons or X-rays. Despite the relative weakness (by a

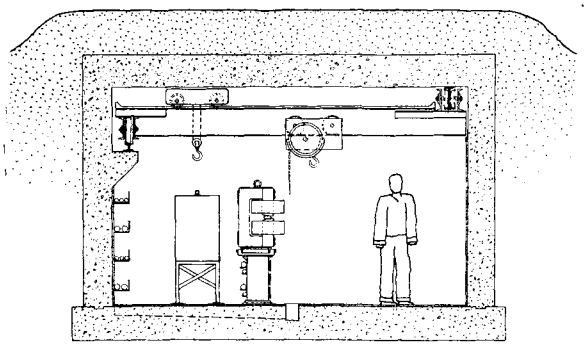

Fig. 18. Cross section through magnet tunnel.

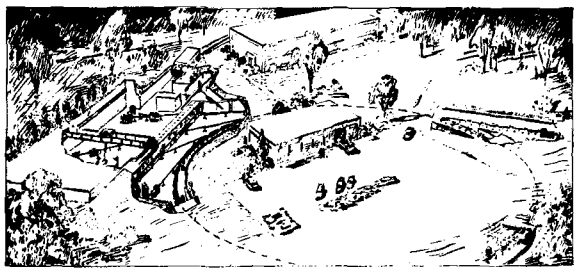

Fig. 19. Artist's conception of accelerator installation.

factor of about 100) of the electromagnetic interactions relative to nuclear interactions, there are excellent reasons for using electrons. As described earlier, electrons can be obtained in high intensity with relative ease and accelerated at constant frequency and at high repetition rates. The effective beam current will be hundreds of times that of a proton machine of equal energy but higher cost. The large fractional on-time makes electronic detection and coincidence experiments easier. Furthermore, the most readily available radiation will be the sharply-collimated beam of X-rays emerging from a target, with a half-angle of only 10^{-3} radians. The high flux density in this beam allows efficient shielding and compact target arrangements, giving large solid angles and low backgrounds in experiments. The opportunity of using small targets may be of great importance in searching for new particles with short half-lives.

We anticipate programs of research in the following general areas :

(*a*) Production and study of proton-antiproton pairs. The threshold for this production reaction with X-rays is at 3.8 Bev; our surplus above threshold result in considerably higher intensities than are available with existing machines.

(*b*) Production of strange new mesons and hyperons and their antiparticles. Our plans for 7.5 Bev are based in part on the desire to exceed the threshold (6.35 Bev) of the reaction producing pairs of "shower particles", the heaviest of all known strange particles in the cosmic radiation.

(*c*) Photoproduction studies of pions, muons and nucleons at higher energies. Extension of data on interaction cross-sections to higher energy will give new information about the relation of mesons to nucleonic and nuclear structure. Furthermore, high intensity beams of much higher energy mesons will become available.

(*d*) Electron structure. The electron or X-ray wavelength in electron-electron or electron-nucleon impacts is short relative to electron or nuclear radii, permitting exploration of charge distribution and structure with considerably better resolution than from existing accelerators. The limits of validity of the laws of relativistic electrodynamics may be tested to these higher energies.

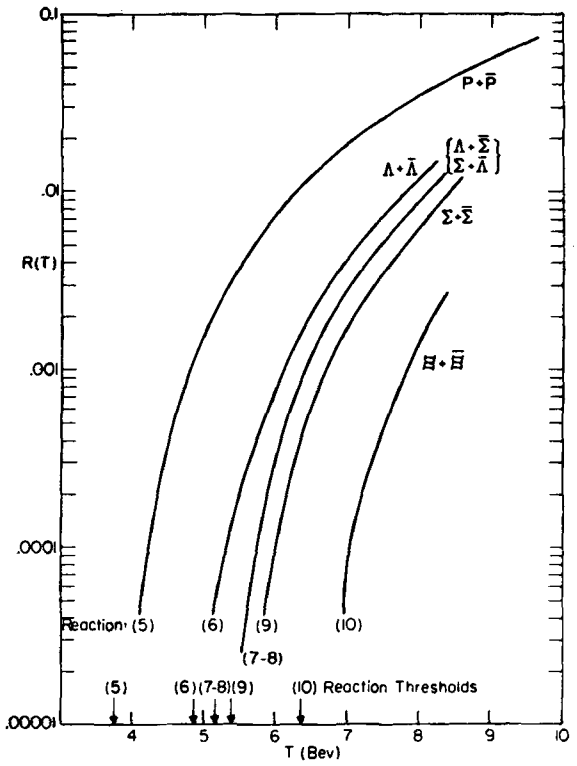

Fig. 21. Estimated relative yields of heavy particle pairs as a function of maximum electron energy.

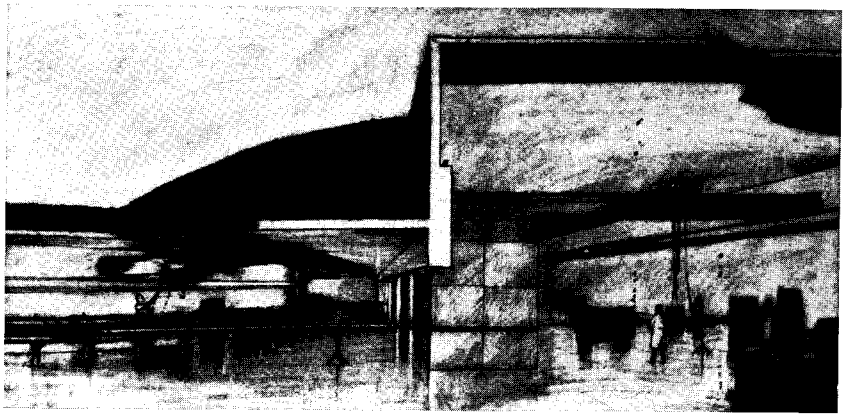

Fig. 20 Artist's conception of interior of target area and experimental area.